JOURNAL OF CATALYSIS 146, 437–448 (1994)

Temperature-Programmed Reduction of Oxidic and Sulfidic Alumina-Supported NiO, WO_3, and NiO–WO_3 Catalysts

P. J. Mangnus,[1] A. Bos, and J. A. Moulijn[2]

Department of Chemical Engineering, University of Amsterdam, Nieuwe Achtergracht 166, 1018 WV Amsterdam, The Netherlands

Received January 13, 1993; revised August 18, 1993

The reduction behaviour of oxidic and sulfidic alumina-supported Ni, W, and NiW catalysts has been studied using temperature-programmed reduction (TPR). Besides giving structural information on the oxidic and sulfidic state, the TPR patterns gave detailed information on the sulfidability of the various oxidic species. From the oxidic species only dispersed NiO was completely sulfidable at 673 K, whereas the other species were partly sulfidable (mixed Ni–W phase, dispersed WO_3, and Ni in the surface alumina layer) or not sulfidable (Ni in subsurface alumina layers and $NiWO_4$). The sulfided catalysts contained at least four types of sulfur, viz. stoichiometric sulfur behaving as S in a bulk analogue (WS_2, Ni_3S_2, NiS_{1+x}) or in NiWS (NiWS is not directly observed under TPR conditions due to sintering into Ni_3S_2 and WS_2), a reactive type of sulfur indicated as S_x, S–H groups, and adsorbed H_2S. Except NiS_{1+x} and S_x, no sulfided phase reduces under HDS conditions. Although hydrogenation of sulfur might well be an elementary step in the desulfurisation reaction, only a weak correlation was observed between the HDS activity and the reduction rate of the S_x species. © 1994 Academic Press, Inc.

INTRODUCTION

Alumina-supported molybdenum and tungsten catalysts, which contain Ni or Co as promoter, are commonly applied for hydrodesulfurisation and hydrodenitrogenation processes. Cobalt-promoted catalysts are mainly used for the removal of sulfur,whereas Ni-promoted catalysts are superior in denitrogenation and hydrogenation reactions. Most studies have been devoted to CoMo and NiMo catalysts. NiW catalysts have not drawn much attention for two reasons: first, they are applied less frequently and, secondly, they may be expected to exhibit similar structural features to the NiMo and CoMo catalysts (W and Mo, and Co and Ni are chemically related). In the relatively few studies devoted to oxidic and sulfidic NiW catalysts, comparable structures to those in CoMo and NiMo catalysts were indeed observed (1–10). However, distinct differences with respect to sulfidability and reducibility of the various species on NiW and CoMo catalysts have also been reported (see Refs. 7, 11–13). Moreover, at high calcination temperatures, the speciation of Ni and Co largely differed in NiW and CoMo catalysts, respectively (7, 12). Since the catalysts are activated by a sulfiding step, it is interesting to study the extent of sulfiding of the various oxidic species and the structure of the catalysts after treatment at commonly applied sulfiding temperatures.

Scheffer *et al.* (14) showed that detailed information on the structure and sulfidability of the various oxidic species can be obtained by the temperature-programmed reduction (TPR) technique. Comparison of the reduction patterns of oxidic and sulfidic catalysts makes it possible to draw conclusions about the sulfidability of the various oxidic species. Since the reduction agent in TPR is hydrogen, the reactivity of the various sulfidic species in TPR are related to the reactivity of these species under hydrotreating conditions. Consequently, it is tempting to investigate whether a relation exists between the reduction rate of the various sulfidic species and the hydrotreating activity of the various catalysts.

EXPERIMENTAL

The model compound nickel(II)sulfide (Johnson Matthey Gmbh) was studied as supplied, whereas tungsten sulfide (Alfa Inorganics Ventron) was treated with H_2S at 673 K, since the sample had been partially reoxidised during storage.

The catalysts were prepared by pore-volume impregnation of a γ-alumina support (Ketjen 000-1.5E high purity, surface area 200 m^2/g, particle size 100–150 $\times$ 10^{-6} m and pore volume 0.5 cm^3/g). The alumina-supported tungsten (W/Al) catalysts were prepared using solutions of ammonium tungstate $(NH_4)_6H_2W_{12}O_{40} \cdot xH_2O$ (Pfaltz and Bauer). After the catalysts were dried at 323 K for 7.2 $\times$ 10^3 s and at 373 K for 54 $\times$ 10^3 s, they were subsequently calcined at 773 K for 7.2 $\times$ 10^3 s in dried air (40 μmol/s). The alumina-supported nickel (Ni/Al) catalysts were

[1] Present address: Akzo Chemicals bv, Nieuwendammerkade 1-3, 1022 AB Amsterdam, The Netherlands.

[2] Present adderss: Faculty of Chemical Technology and Materials Science, Delft University of Technology, Julianalaan 136, 2628 BL Delft, The Netherlands.

0021-9517/94 $6.00

TABLE 1

Alumina-Supported Tungsten (W/Al), Nickel (Ni/Al), and Nickel–Tungsten (Ni/W/Al) Catalysts

Catalyst code	Weight content (%) NiO	WO_3
W(2.4)/Al	—	15.6
Ni(0.85)/Al	2.0	—
Ni(1.7)/Al	4.0	—
Ni(2.6)/Al	6.0	—
Ni(1.0)/W(2.3)/Al	2.0	15.2
Ni(2.0)/W(2.3)/Al	4.0	14.9
Ni(2.9)/W(2.3)/Al	5.8	14.6

prepared by successive additions of the equivalent of 2 wt.% NiO by pore-volume impregnation of $Ni(NO_3)_2 \cdot 6H_2O$ (Janssen Chimica). After each impregnation step, the catalysts were dried and calcined in a procedure similar to that described for the W/Al catalysts. After the final impregnation step, the catalysts were calcined at 773 or 1073 K. The Ni–W/Al catalysts were prepared in the same way starting from W/Al catalysts containing 15.6 wt.% WO_3. The catalysts are denoted by the number of metal atoms per nm^2 of initial support area, followed by the temperature of calcination, e.g., Ni(2.9)/W(2.3)/Al-773 contains 5.8 wt.% NiO and 14.6 wt.% WO_3, and was calcined at 773 K. The catalysts are listed in Table 1.

The TPR-S equipment has been described in detail elsewhere (14, 15). Preceding the reduction step, the catalysts have been sulfided *in situ* in a mixture of 15 vol% H_2S in H_2. The sulfiding procedure consisted of the following steps. After flushing the quartz reactor with Ar at room temperature for 900 s, the reactor was switched to the sulfiding mixture. After sulfiding at room temperature for 900 s, the reactor temperature was raised to the final temperature with a heating rate of 0.167 K/s. All catalysts were sulfided at 673 K except for W(2.4)/Al which was sulfided at various temperatures. After sulfiding (673 K, 7.2×10^3 s), the reactor was switched to purified Ar and purged for 1.8×10^3 s. Subsequently, the reactor was cooled to room temperature. When higher sulfiding temperatures were applied, the reactor was cooled to 673 K in the sulfiding mixture and subsequently purged in Ar, as described above. The W(2.4)/Al catalyst, which was sulfided at 573 K, was purged at this temperature for 1.8×10^3 s and subsequently cooled to room temperature. As soon as the reactor reached ambient temperature (after about 600 s) the reactor was switched to H_2/Ar (67 vol% H_2 in Ar). When the TCD signal was stabilised ($3.6–7.2 \times 10^3$ s) the sample was reduced at a heating rate of 0.167 K/s up to 1270 K. The H_2S production was detected with a UV-spectrophotometer (Perkin–Elmer C75, set at 195 nm). The H_2 partial pressure was measured after H_2S and H_2O were trapped in an oxidic CoMo/Al catalyst and a molecular sieve, respectively. Since organic material adsorbs on the catalysts (16), a FID detector was applied to measure the CH_4 production. In quantitative analyses the TCD signal was corrected for the CH_4 peaks.

To distinguish between reduction of sulfidic and oxidic samples the abbreviations TPR-S and TPR are used for temperature programmed reduction of sulfidic and oxidic catalysts, respectively. The TPR experiments were carried out similarly to TPR-S.

RESULTS

Bulk Compounds

NiS. The TPR-S pattern of NiS is shown in Fig. 1a. The H_2 consumption and H_2S production are closely matched. The patterns are dominated by two large peaks, viz., a peak between 600 and 900 K (maximum at 790 K) and a broad peak between 900 and 1270 K. The second peak shows a distinct shape since the reduction rate slowly increased up to 1200 K and then suddenly decreased to nil in a short period of time. Two small peaks are superimposed on these large peaks at about 840 and 970 K. The total H_2S production and H_2 consumption agreed with complete reduction of NiS to Ni^0.

WS_2. The TPR-S pattern of WS_2 is shown in Fig. 1b. Most of the reduction took place between 1000 and 1270 K; the reduction rate increased exponentially up to 1270 K, stayed nearly constant, and suddenly dropped to zero upon depletion of S (not shown). The H_2 consumption

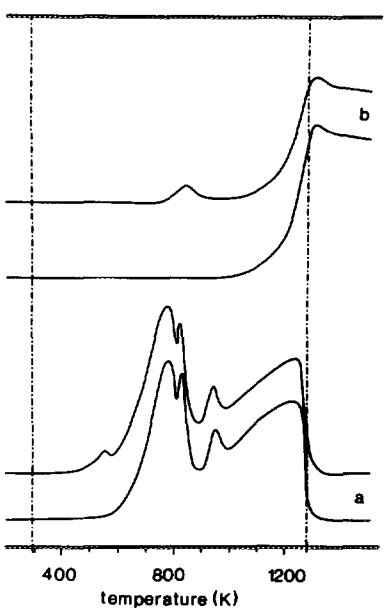

FIG. 1. TPR-S patterns of model compounds. (a) NiS, (b) WS_2. UV signal (lower curve) and TCD signal (upper curve) are shown.

and H_2S production were equal in this temperature region. The small H_2 consumption peak observed around 820 K is ascribed to the reduction of an oxidic species since no H_2S production is observed simultaneously.

The TPR patterns of the model compounds NiO, WO_3, $NiAl_2O_4$, $Al_2(WO_4)_3$, and $NiWO_4$ have already been presented elsewhere (7).

Catalysts

Combination of TPR and TPR-S allows a detailed discussion on the sulfidability of the various phases present. TPR measurements of Ni/Al and Ni/W/Al have been reported before by Scheffer *et al.* (7). However, since the detailed structure of the Ni catalysts strongly depends on the method of preparation, the TPR patterns of Ni/Al and Ni/W/Al catalysts are also included.

The TPR-S patterns are divided into three regions, viz. I, II, and III. Region I encloses the temperature region up to 500–600 K, region II the temperature region from 500–600 K to 800–900 K, and region III ranges from 800–900 K up to the end of the temperature program.

W(2.4)/Al. The TPR patterns were in agreement with earlier results (7, 17). Reduction of the WO_3 species takes place between 1050 and 1270 K. Since these TPR patterns are hardly affected by the preparation procedure, they are not included in this paper.

The TPR-S patterns of W(2.4)/Al, sulfided at various temperatures, are shown in Fig. 2. In all cases the H_2S production is lower than the H_2 consumption. This difference decreases for catalysts sulfided at higher temperatures. In Table 2, it is shown that an increase of the sulfiding temperature from 573 to 873 K resulted in an increase of the degree of sulfiding from 24 to 95%. The peak maximum of both TCD and UV peaks in region III shifted to higher temperatures with increasing sulfiding temperature.

The amount of H_2S producted in region II was in all cases larger than the H_2 consumption; both signals decreased with increasing sulfiding temperature. A third H_2S production and associated H_2 consumption peak are observed in region I (about 440 K). These peaks are ascribed to a reduction process ($H_2 + S \rightleftarrows H_2S$). The intensity of the peak increased with increasing sulfiding temperature. A fourth peak is observed below 400 K. Since no H_2 consumption is observed in this temperature region, the H_2S production is ascribed to a desorption process.

Ni(x)/Al. By comparison of the TPR and TPR-S patterns which are shown in Figs. 3 and 4, respectively, the sulfidability of the various oxidic species can be determined reliably. Quantitative TPR data are given in Table 3. In the TPR-S patterns of the three Ni(x)/Al-773 catalysts, the TCD signal (H_2) is much larger than the UV signal (H_2S), showing that a large fraction of the NiO is

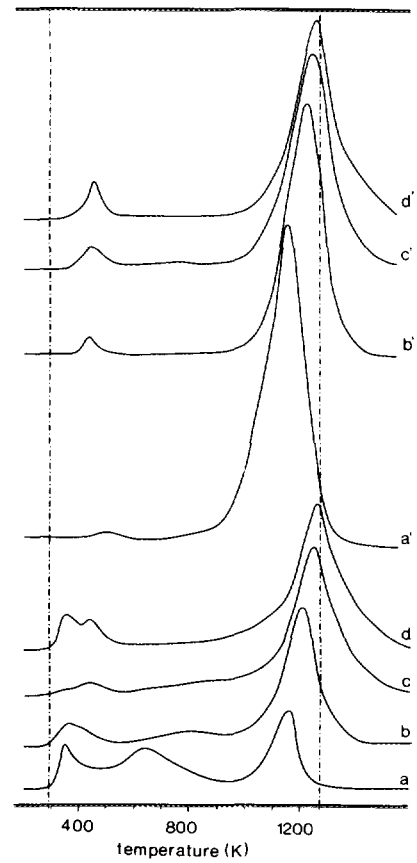

FIG. 2. TPR-S pattern of W(2.4)/Al-773 sulfided at various temperatures. (a) $T_{sulf.}$ = 573 K, (b) $T_{sulf.}$ = 673 K, (c) $T_{sulf.}$ = 773 K, (d) $T_{sulf.}$ = 873 K. UV signal (lower curves, a–d) and TCD signal (upper curves, a'–d') are shown.

not sulfidable at 673 K, which is the upper limit of common sulfiding temperatures. Comparison of the TPR and TPR-S patterns shows that the H_2 peak around 1000–1100 K is not changed upon sulfiding. In contrast, the height of the H_2 peak between 650 and 850 K decreased as a result of sulfiding, but did not disappear completely. Table 3 shows that the total amount of H_2S produced in regions II and III is at most 50% of the amount of H_2 consumed.

A striking feature in the TPR-S patterns is a TCD peak at about 500 K which is absent in the TPR spectra. This H_2 peak is accompanied by a H_2S peak of comparable size. The peak heights both increased with increasing NiO content, but normalized to the amount of Ni they decreased.

The H_2 consumption peak below 800 K in the TPR pattern, which was coupled to a FID signal, is ascribed to the reduction of organic material adsorbed on the surface of the catalyst. This finding illustrates that it is necessary to use a FID detector besides a TCD.

The TPR and TPR-S patterns of the Ni(x)/Al-1073 are shown in Figs. 5 and 6, respectively. They differ profoundly from the catalysts calcined at 773 K. Remarkably,

TABLE 2
H_2S Production and H_2 Consumption in TPR-S of W(2.4)/Al Catalysts Sulfided at Varying Temperature

Catalysts	Sulf. temp (K)	Amount W (μmol)	Region I (μmol)		Region II (μmol)		Region III (μmol)		Sulf.[a] (%)
			H_2S	H_2	H_2S	H_2	H_2S	H_2	
W(2.4)/Al-773	573	67	8.7	~0	41	~0	29	182	24
W(2.4)/Al-773	673	67	12	3.6	16	~0	88	153	67
W(2.4)/Al-773	773	67	6.6	7.0	15	~0	108	141	83
W(2.4)/Al-773	873	67	17	8.1	~0	~0	126	137	95

Note. The data are normalised to 0.1 g of catalyst.

[a] The degree of sulfiding is calculated based on the amount of H_2S produced and H_2 consumed in temperature region III, as follows: sulfiding degree = $100(1 - ((x - y)/3z))$; x = amount of H_2, y = amount of H_2S, z = amount of W.

in temperature region III the TCD signal of the TPR and TPR-S patterns are exactly the same and no H_2S production is observed in the TPR-S pattern. Analogous to the TPR-S patterns of Ni(x)/Al-773, a UV and TCD signal are observed in temperature region I. However, they differ in two respects: (i) the UV signal consists of two peaks, one of which coincided with a TCD peak and (ii) the peaks are smaller.

Ni(x)/W(2.3)/Al. The TPR and TPR-S patterns of the Ni(x)/W(2.3)/Al-773 catalysts are shown in Figs. 7 and 8, respectively. The quantitative data of the TPR-S measurements are listed in Table 4.

The TPR-S patterns show that the integrated H_2 consumption is larger than the H_2S production for all three catalysts, showing that none of the catalysts is completely sulfided at common sulfiding temperatures (<673 K). In temperature region III two overlapping peaks are present, one at 1200 K and the other around 1050 K. It is striking that the H_2S production at 1200 K is independent of the Ni content whereas the H_2 consumption decreases with increasing Ni content. The height of both the H_2S and H_2 peaks around 1050 K increases with increasing Ni content. Similar to the W(2.4)/Al-773 catalyst, the amount of H_2S produced in region II is higher than the corresponding H_2 consumption. In region I a H_2 consumption and H_2S production peak are observed at 410 K (similar peaks are located at about 440 and 500 K for W(2.4)/Al and Ni(x)/Al, respectively).

The TPR and TPR-S patterns of the Ni(x)/W(2.3)/Al-1073 catalysts are shown in Figs. 9 and 10, respectively. The quantitative data of the TPR-S measurements are

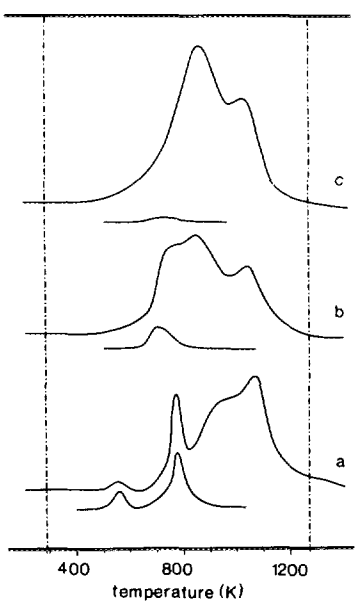

FIG. 3. TPR patterns of Ni(x)/Al-773 catalysts. (a) Ni(0.85)/Al-773, (b) Ni(1.7)/Al-773, (c) Ni(2.6)/Al-773. FID signal (lower curve) and TCD signal (upper curve) are shown.

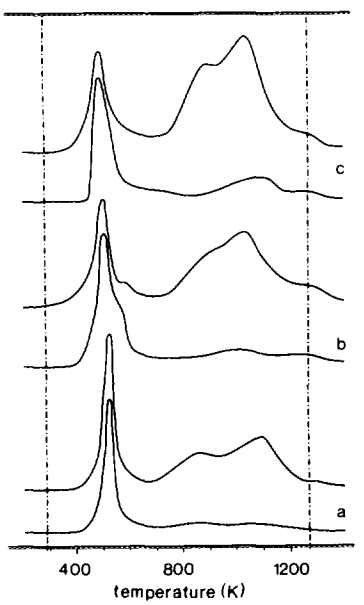

FIG. 4. TPR-S patterns of Ni(x)/Al-773 catalysts sulfided at 673 K. (a) Ni(0.85)/Al-773, (b) Ni(1.7)/Al-773, (c) Ni(2.6)/Al-773. UV signal (lower curve) and TCD signal (upper curve) are shown.

TABLE 3

H_2S Production and H_2 Consumption in TPR-S of Sulfided Ni(x)/Al Catalysts Calcined at 773 and 1073 K

Catalysts	Sulf. temp (K)	Amount Ni (μmol)	Region I (μmol)		Region II (μmol)		Region III (μmol)		Sulf.[a] (%)
			H_2S	H_2	H_2S	H_2	H_2S	H_2	
Ni(0.8)/Al-773	673	27	12	13	6.4	~0[b]	6.0	23	24
Ni(0.8)/Al-1073	673	27	12	2.9	~1.2	~0	~0	30	~0
Ni(1.7)/Al-773	673	53	19	15	~0	~0[b]	17	45	48
Ni(1.7)/Al-1073	673	53	13	8.4	1.9	~0	~0	53	~0
Ni(2.6)/Al-773	673	80	17	19	8.2	~0[b]	26	59	54
Ni(2.6)/Al-1073	673	80	12	8.9	4.1	~0	~0	80	~

Note. The data are normalised to 0.1 g of catalyst.

[a] The degree of sulfiding is calculated based on the amount of H_2S produced and H_2 consumed in temperature region III, as follows: sulfiding degree = $100(1 - ((x - y)/z))$; x = amount of H_2, y = amount of H_2S, z = amount of Ni.

[b] The H_2 consumption between 700 and 800 K is included in region III.

collected in Table 4. On the basis of these data it is concluded that calcination at 1073 K strongly decreased the sulfidability of these catalysts. By comparing the TPR-S and TPR patterns it is clear that sulfiding at the higher temperatures results in a decrease of the TCD signal at 1200 K while between 1050 and 1100 K, it only slightly decreased. With increasing Ni content, the H_2S production peak at 1200 K decreased whereas the H_2S production at about 1050 K increased. The H_2S production in region II is larger than the associated H_2 consumption. In region I of the TPR-S pattern a H_2 consumption and an associated H_2S production are observed at about 430 K.

DISCUSSION

Clearly, the system is quite complex. The TPR patterns strongly depend on the specific pretreatment conditions and the loading of the catalysts. Use of both TCD and FID detectors enables correction to be made of the patterns for hydrogenation of carbonaceous material, which is always

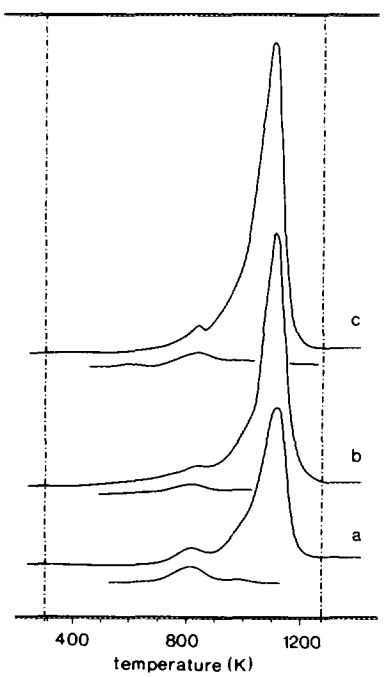

FIG. 5. TPR patterns of Ni(x)/Al-1073 catalysts. (a) Ni(0.85)/Al-1073, (b) Ni(1.7)/Al-1073, (c) Ni(2.6)/Al-1073. FID signal (lower curve) and TCD signal (upper curve) are shown.

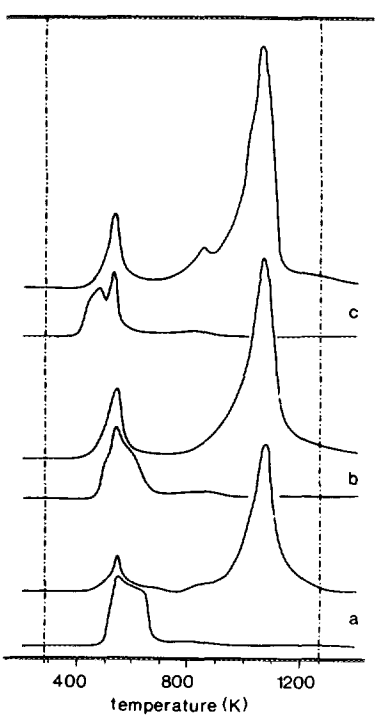

FIG. 6. TPR-S of Ni(x)/Al-1073 catalysts sulfided at 673 K. (a) Ni(0.85)/Al-1073, (b) Ni(1.7)/Al-1073, (c) Ni(2.6)/Al-1073. UV signal (lower curve) and TCD signal (upper curve) are shown.

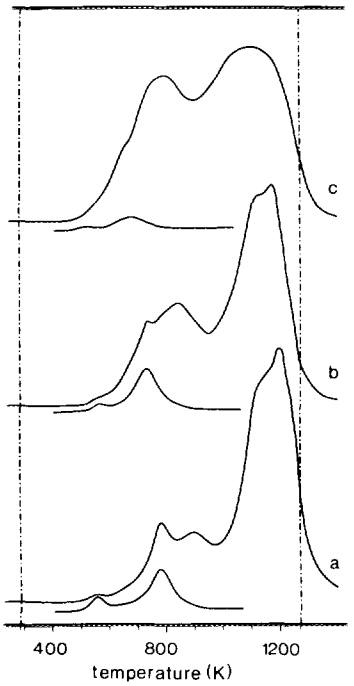

FIG. 7. TPR patterns of Ni(x)/W(2.3)/Al-773 catalysts. (a) Ni(1.0)/W(2.3)/Al-773, (b) Ni(2.0)/W(2.3)/Al-773, (c) Ni(2.9)/W(2.3)/Al-773. FID signal (lower curve) and TCD signal (upper curve) are shown.

present. In TPR-S the H_2S and H_2 were detected by a UV and TCD detector, respectively. In this way the patterns can be resolved into the different processes occurring:

(i) H_2S desorption (UV signal without TCD signal).
(ii) –S– hydrogenation (UV signal associated with a TCD signal).
(iii) –O– hydrogenation (TCD signal, no UV signal).
(iv) C hydrogenation (TCD signal associated with FID signal, no UV signal).

Bulk Compounds

NiS. Several nickel sulfides can be formed when NiS is exposed to hydrogen, viz., Ni_6S_5, Ni_3S_2, and $Ni_3S_{2\pm x}$ (18). Deconvolution of the complex patterns is not straightforward, but it does not disagree with reduction of NiS to Ni_3S_2 below 850 K and subsequent reduction to Ni^0 in the high temperature region. It was shown by Scheffer *et al.* (14) and Mangnus *et al.* (15) that the reduction of metal sulfides under commonly applied TPR conditions is in many cases determined by thermodynamics. To check whether this is the case here, the H_2S/H_2 ratio at various temperatures during TPR-S was compared with the H_2S/H_2 ratios at which NiS and Ni_3S_2, and Ni_3S_2 and Ni are at thermodynamic equilibrium. In Fig. 11, the experimentally determined H_2S/H_2 ratios are plotted together with the equilibrium values reported by Rosenqvist (18). It is clear that the first step (NiS to Ni_3S_2) is determined by kinetics while the second step (Ni_3S_2 to Ni^0) is determined by thermodynamics. These conclusions indicate that our deconvolution procedure was correct.

WS_2. The reaction observed above 1000 K is due to the reduction of WS_2 to W. This is not surprising since no intermediate sulfides are known to exist between WS_2 and W. To verify whether the reduction was determined by the thermodynamics, the equilibrium data were calculated (19). Figure 12 shows that the experimental points (curve a) are situated close to the calculated line (curve c), proving that reduction of WS_2 is determined by thermodynamics under TPR-S conditions. This is analogous to reduction of MoS_2. Because the small H_2 consumption peak around 810 K is observed in the same temperature region where the reduction of WO_3 took place (17), it is ascribed to the reduction of WO_3 formed by reoxidation during storage. The fact that part of the WO_3 survived the resulfiding step at 673 K indicates that the reoxidation was not restricted to the surface layers.

Catalysts

W(2.4)/Al. The experimental H_2S/H_2 ratio under TPR-S conditions of W(2.4)/Al which was sulfided at 873 K is plotted in Fig. 12 (curve b). Above 1000 K, it is situated closely to the curve corresponding with the ther-

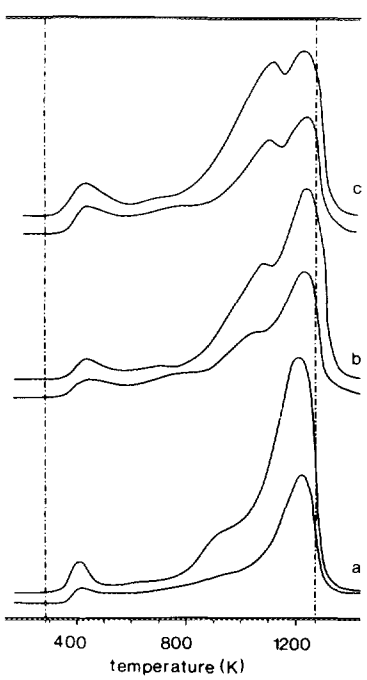

FIG. 8. TPR-S patterns of Ni(x)/W(2.3)/Al-773 catalysts which are sulfided at 673 K. (a) Ni(1.0)/W(2.3)/Al-773, (b) Ni(2.0)/W(2.3)/Al-773, (c) Ni(2.9)/W(2.3)/Al-773. UV signal (lower curve) and TCD signal (upper curve) are shown.

TABLE 4

H_2S Production and H_2 Consumption in TPR-S of Sulfided Ni(x)/W(2.3)/Al Catalysts Calcined at 773 and 1073 K

Catalyst	Sulf. temp (K)	Amount (μmol)		Region I (μmol)		Region II (μmol)		Region III (μmol)		Sulf.[a] (%)
		Ni	W	H_2S	H_2	H_2S	H_2	H_2S	H_2	
Ni(1.0)/W(2.3)/Al-773	673	27	63	2.4	7.1	12	13	73	146	51
Ni(1.0)/W(2.3)/Al-1073	673	27	63	5.1	4.5	16	~0	56	168	39
Ni(2.0)/W(2.3)/Al-773	673	54	61	5.3	5.8	20	10	105	170	66
Ni(2.0)/W(2.3)/Al-1073	673	54	61	4.8	4.8	18	~0	60	188	38
Ni(2.9)/W(2.3)/Al-773	673	78	60	8.9	10	24	18	112	174	65
Ni(2.9)/W(2.3)/Al-1073	673	78	60	7.0	6.3	16	6.8	50	223	29

Note. The data are normalised to 0.1 g of catalyst.

[a] The degree of sulfiding is calculated as follows: sulfiding degree = $100(x/(2y + 2/3z))$, x = H_2S production in region III, y = amount of W, z = amount of Ni.

modynamic equilibrium of WS_2 and W^0. This is remarkable, because from the results of Breysse *et al.* (20), it is reasonable to assume that on the catalysts studied, WS_2 slabs are present with very limited degree of stacking. Apparently, in spite of the high dispersion, WS_2 slabs behave like bulk WS_2. The underlying reason might be that bulk WS_2 consists of "WS_2" layers, which are only weakly bonded to each other. Consequently, a single slab behaves quite similarly to the bulk. The shift of the reduction maximum towards higher temperatures when the sulfiding temperature is increased is due to the presence of different amounts of WS_2 on these catalysts (the higher the sulfiding temperature, the larger the amount of WS_2) and not to a different slab size or interaction strength

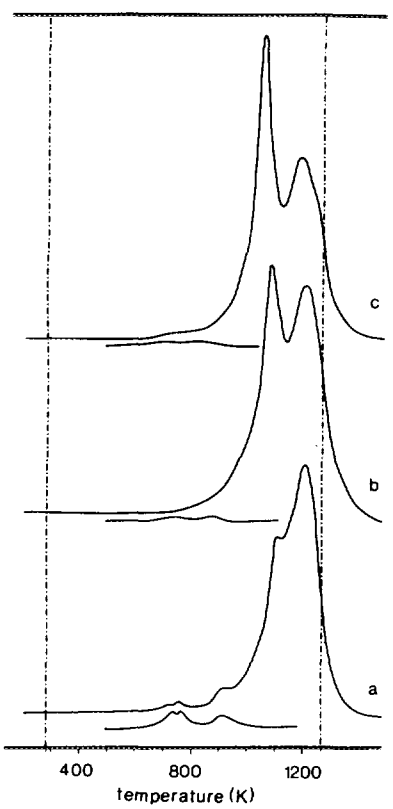

FIG. 9. TPR patterns of Ni(x)/W(2.3)/Al-1073 catalysts. (a) Ni(1.0)/W(2.3)/Al-1073, (b) Ni(2.0)/W(2.3)/Al-1073, (c) Ni(2.9)/W(2.3)/Al-1073. FID signal (lower curve) and TCD signal (upper curve) are shown.

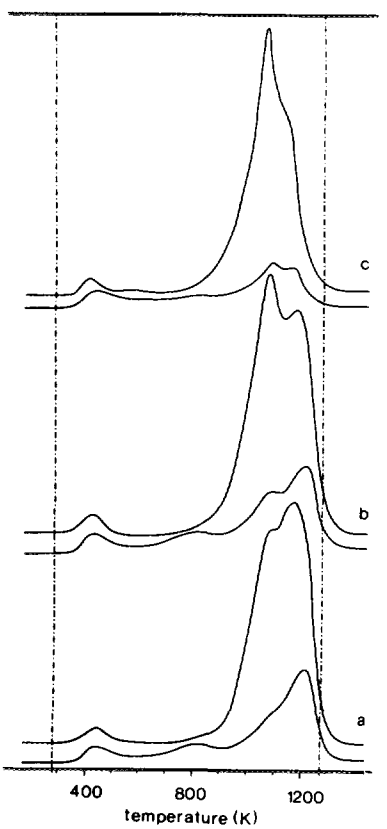

FIG. 10. TPR-S patterns of Ni(x)/W(2.3)/Al-1073 catalysts sulfided at 673 K. (a) Ni(1.0)/W(2.3)/Al-1073, (b) Ni(2.0)/W(2.3)/Al-1073, (c) Ni(2.9)/W(2.3)/Al-1073. UV signal (lower curve) and TCD signal (upper curve) are shown.

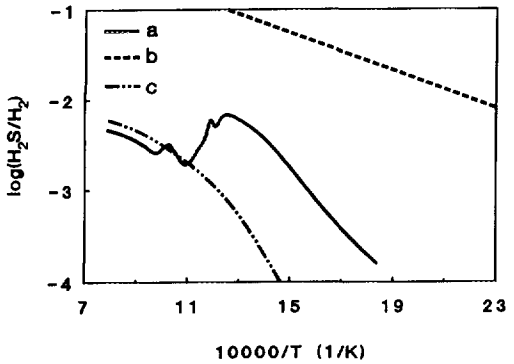

FIG. 11. Comparison of the H_2S/H_2 ratio during the TPR-S experiments of NiS (a) with the H_2S/H_2 ratio at thermodynamic equilibrium of NiS and Ni_3S_2 (b) and Ni_3S_2 and Ni^0 (c). The curve for the reduction of NiS to Ni_3S_2 is extrapolated to lower temperatures.

of the WS_2 slabs with the support. This illustrates the necessity of carrying out thermodynamic calculations to avoid errors that are easily made.

As the reduction above 1000 K is ascribed to the reduction of the WS_2 slabs, the degree of sulfiding is calculated on the basis of the amount of H_2 consumed and H_2S produced in this temperature region. The low degree of sulfiding ($WS_{0.48}$) after sulfiding at 573 K agrees with the literature (8). After sulfiding at 873 K, the S/W ratio approached the stoichiometric ratio of 2. As already suggested previously (8), the low sulfiding rate of the alumina-supported WO_3 species is due to their strong interaction with the support.

The experimental H_2S/H_2 ratios below 1000 K are higher than at equilibrium, confirming that the H_2S produced below this temperature is not due to reduction of stoichiometric WS_2. From the fact that in region II the H_2S production is larger than the H_2 consumption we conclude that the H_2S produced in this region is due to recombination of S–H groups and reaction of S–H groups with hydrogen. The presence of S–H groups on similar catalysts is supported by Raman spectroscopy (21). The large amount of S–H groups on the catalysts which were sulfided at low temperatures (573 and 673 K) suggests that S–H groups are formed on oxidic or oxysulfidic species. At higher sulfiding temperatures smaller amounts of S–H groups are present, probably because they recombine, resulting in the formation of H_2S while a sulfur ion is left behind in the oxysulfidic structure (21, 22).

The H_2 consumption and H_2S production observed at about 440 K is ascribed to the reduction of a nonstoichiometric sulfur species. Such a reactive type of sulfur has been reported previously (14, 15, 23), and has been referred to as S_x. It was concluded that these sulfur species were chemisorbed on coordinatively unsaturated sites. It is interesting that the amount of S_x increased with increasing sulfiding temperature. Due to the increased degree of sulfiding at higher temperatures, the number of WS_2 slabs increased and apparently simultaneously the amount of coordinatively unsaturated edge/corner sites increased.

Ni(x)/Al. For a detailed description of the structure of NiO/Al catalysts we refer to papers by Scheffer *et al.* (7, 9), Puxley *et al.* (24), and de Korte *et al.* (25). Since the structure of these catalysts has been studied in detail with TPR (7), the various reduction peaks are assigned without extensive discussion. In the TPR patterns of the Ni(x)/Al calcined at 773 K the peaks have been assigned to species as follows:

(a) The reduction peak between 700 and 1000 K is ascribed to a highly dispersed NiO surface phase (in Refs. 7 and 9 referred to as phase II). The width of this peak suggests a rather poorly defined phase consisting of Ni species with a small, variable amount of Al^{3+} neighbours. The Ni ions are octahedrally coordinated.

(b) The peak between 1000 and 1200 K is ascribed to reduction of highly disperse NiO with a stoichiometry close to $NiAl_2O_4$. Compared to the disperse NiO phase, these Ni ions are surrounded by a higher number of Al^{3+} ions (in Refs. 7 and 9, denoted as phase IIIa). Since the calcination temperature of 773 K is too low for extensive diffusion, the Ni^{2+} ions are located at the surface. Using diffuse reflectance spectroscopy it has been shown that these Ni ions are octahedrally coordinated (9).

Calcination at 1073 K resulted in the disappearance of the highly dispersed NiO surface species. The sharp peak around 1170 K indicates that Ni is present in a rather well-defined phase. It is concluded that calcination at 1073 K causes extensive diffusion of Ni into the alumina lattice, resulting in a diluted $NiAl_2O_4$ phase, and both octahedrally and tetrahedrally coordinated Ni ions are formed (in Refs. 7 and 9 denoted as phase IIIb). The absence of a reduction peak at about 600 K indicates that no large NiO crystallites were present on any of these catalysts (7).

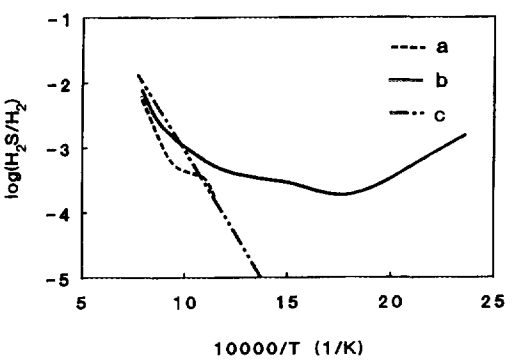

FIG. 12. Comparison of the actual H_2S/H_2 ratio during the TPR-S experiments of WS_2 (a) and W(2.4)/Al (b) sulfided at 873 K with the theoretical H_2S/H_2 ratio at thermodynamic equilibrium of WS_2 with W metal (c).

Comparison of the TPR and TPR-S patterns directly shows that Ni present in the diluted $NiAl_2O_4$ phase (phase IIIb) is not sulfidable while Ni present in the surface $NiAl_2O_4$ phase (phase IIIa) is hardly sulfidable. The fact that the diluted $NiAl_2O_4$ phase is not sulfidable at industrially common sulfiding temperatures has also been reported by others (8, 26). Because diffusion of the Ni ions back to the surface layer is very slow at these temperatures, sulfiding is excluded.

The major part of the surface $NiAl_2O_4$ species (phase IIIa) is not sulfidable at generally applied sulfiding conditions. Apparently, the O–S exchange, essential for sulfiding, is not possible, probably because all oxygen atoms surrounding the Ni are also coordinated to the Al^{3+} ions.

After sulfiding at 673 K the reduction peak of the dispersed NiO surface species has nearly completely disappeared, indicating that this phase is easy to sulfide. On the basis of the Ni–S phase diagram (18) it is expected that the NiO species are sulfided to NiS_{1+x}. Formation of NiS, under comparable sulfiding conditions, has also been reported elsewhere (8, 10). On the basis of the quantitative data (H_2 consumption and H_2S production), it is concluded that after sulfiding the major part of the sulfided Ni species was present as NiS_{1+x} microcrystallites. Analogous to bulk NiS, reduction of these crystallites took place in two steps, viz. the first step of NiS_{1+x} to Ni_3S_2 at 500 K and the second step Ni_3S_2 to Ni^0 above 800 K. On the basis of TPS measurements, Scheffer *et al.* (8) concluded that two types of sulfided Ni species were present, viz., NiS_{1+x} microcrystallites and ultra-dispersed sulfided NiO species stabilised by Ni–O–Al links against sintering and reduction. The latter will not reduce in two steps as observed for crystallites. The percentage of Ni present as dispersed sulfided NiO species cannot be deduced from these patterns. Thermodynamic analysis shows that Ni_3S_2 particles and dispersed nickel sulfide species are more stable than bulk Ni_3S_2. Apparently, they are small enough to experience significant active phase support interaction causing an increased stability.

The amount of H_2S produced at low temperatures (500 K) is larger than the amount calculated according to the reduction of NiS_{1+x} into Ni_3S_2. Probably, the 500 K peak is the result of reduction of both NiS_{1+x} and chemisorbed S species, similar to the S_x species observed for the W(2.4)/Al-773 catalyst. As the reduction of these S_x species is also observed on the nonsulfidable Ni(x)/Al-1073 catalysts, we conclude that chemisorption of these sulfur species is not restricted to sulfided Ni but can also take place on coordinatively unsaturated oxidic Ni species. The increase of the amount of S_x with increasing Ni content on these catalysts confirms that the S species adsorb on exposed Ni ions rather than on the support. Figure 6 shows that for the catalysts calcined at 1073 K the reduction of these sulfur species is taking place at 540 K instead of 500 K as observed on the catalysts calcined at 773 K. The shift of the reduction temperature probably reflects the stronger interaction of the S_x species with the oxidic catalyst: the Ni ions in the surface $NiAl_2O_4$ layer are polarised by Al^{3+} ions, resulting in a stronger interaction with the adsorbed sulfur atoms. These S_x species are formed by decomposition of H_2S on the coordinatively unsaturated Ni ions.

Ni(x)/Al. Alumina-supported $NiO–WO_3$ catalysts have been studied in detail by TPR by Scheffer *et al.* (7). Hence, assignment of the various TPR peaks is based partly on their interpretation (7). At least four phases which reduce in three different temperature regions are detected on the catalysts calcined at 773 K as summarised in the following:

(a) The peak between 700 and 1000 K, which was also observed during the reduction of the Ni(x)/Al-773 catalysts, is ascribed to the reduction of the highly dispersed NiO surface species. The presence of this phase is not surprising since at a loading of 2.3 at/nm^2 not all the alumina is covered with WO_3 (a monolayer is formed at a W loading of approx. 4.3 at/nm^2) (2).

(b) The peak between 950 and 1100 K is due to the reduction of surface $NiAl_2O_4$ (phase IIIa). In addition, the reduction of a mixed $NiO–WO_3$ phase (indicated as NiWOAl by Scheffer *et al.* (7, 9)) takes place in this temperature region. The presence of such a ternary compound has also been reported by others (2, 28).

(c) The peak at about 1200 K is ascribed to the reduction of the WO_3 monolayer, and the decreased intensity with increasing NiO content indicates that part of the WO_3 species reduced at lower temperatures. This is not surprising since incorporation of Ni in the WO_3 monolayer results in a decrease of the number of Al neighbours of the W ions which causes a more easy reduction of a part of the WO_3 species. The TPR peak is accordingly very broad, as expected for such an ill-defined structure with varying coordination.

Calcination of these catalysts at 1073 K resulted in the following changes:

(i) The peak between 700 and 1000 K disappeared completely, obviously because the dispersed NiO phase reacted into a more stable phase.

(ii) Between 1050 and 1100 K, a sharp peak is observed which is ascribed to the reduction of $NiWO_4$. The sharpness of this latter peak suggests a well-defined phase. Since XRD did not reveal any crystalline phase it is concluded that Ni is present in microcrystalline $NiWO_4$ particles. In agreement herewith, the intensity of the reduction peak of the WO_3 monolayer species at 1200 K is strongly decreased. The formation of $NiWO_4$ microcrystallites, at higher calcination temperatures, was also observed by

Iannibello *et al.* (29). Scheffer *et al.* (7) have reported that the formation of this phase is thermodynamically more favourable than the formation of $NiAl_2O_4$.

The TPR-S patterns are quite complex. It is easiest to start the discussion with the highest temperature peak. Both the TCD and UV peak are also found in the TPR-S patterns of W/Al. The peaks at the highest temperature (1200 K) are due to reduction of WS_2 and WO_3. The height of the H_2S peak is only slightly affected by the presence of Ni, indicating that the sulfiding degree of the WO_3 species is not altered significantly. Only part of the tungsten (WO_3 and WS_2) is reduced in this peak, the other part being reduced in the peak at 1050 K. Since all sulfided W species reduce at about 1200 K, the W species that are reduced at 1050 K should be in their oxidic state. We conclude that W is here present as a mixed nonsulfided Ni–W phase (NiWOAl), also because with increasing Ni content this peak increases while the highest temperature TCD peak decreases.

The H_2S production peak with a maximum between 900 and 1100 K is ascribed to a contribution of the reduction of nickel sulfide and Ni located at the edges of WS_2 slabs. In analogy with "CoMoS" we denote these species as NiWS. The experimental H_2S/H_2 ratios are compared with the thermodynamic data with respect to $NiS \rightarrow Ni_3S_2$ and $Ni_3S_2 \rightarrow Ni$ in Fig. 13. Remarkably, the points of the peak between 900 and 1100 K are situated close to the reduction curve of Ni_3S_2. Apparently, reduction of Ni_3S_2 is taking place. At first sight this is surprising, because it is generally accepted that sulfiding of supported CoMo, NiMo, CoW, and NiW catalysts results in the formation of the so-called CoMoS, NiMoS, CoWS, and NiWS phases, respectively. Since the precursor of the NiWS phase, the NiWOAl phase, was present on the catalyst, we may assume that a large part of the Ni was present as NiWS after sulfiding. It is quite striking that no separate reduction peak of Ni situated on the edges of the WS_2 slabs is observed; it is certainly not expected, a priori, that the reduction behaviour of the NiWS phase would be similar to Ni_3S_2. This contradiction can be explained as follows. Before the reduction temperature of this phase is reached, sintering occurs, resulting in the formation of Ni_3S_2 and WS_2, and, hence, in a strong decrease of the amount of NiWS. Deconvolution of the Ni_3S_2 and WS_2 peaks indicates a slight increase of the amount of sulfidable Ni species compared to Ni in the Ni(x)/Al-773 catalysts. Apparently, part of the Ni present in the NiWOAl phase is better sulfidable than Ni surface and subsurface spinels in Ni(x)/Al catalysts. However, as was already mentioned, a part of this NiWOAl phase is not sulfidable at 673 K. Most probably, NiO species present on the WO_3 monolayer are easily sulfidable whereas the sulfidability of the Ni species is low when these ions are incorporated in the WO_3 monolayer. This conclusion is supported by the TPR-S measurements of the Ni(x)/W(2.3)/Al catalysts calcined at 1073 K. The degree of sulfiding of these catalysts decreased significantly, although Ni and W species were still present as dispersed phases (no XRD peaks from crystalline NiO, WO_3, or $NiWO_4$). The degree of sulfiding of the Ni and W species became even lower than that of the monometallic catalysts. Since the $NiWO_4$ is not sulfided at 673 K, it is plausible that sulfiding of Ni is strongly retarded by incorporation in the WO_3, monolayer. Results of Scheffer *et al.* (8), who showed that $NiWO_4$ sulfided only above 900 K, agree with our conclusion that $NiWO_4$ is not sulfidable at 673 K.

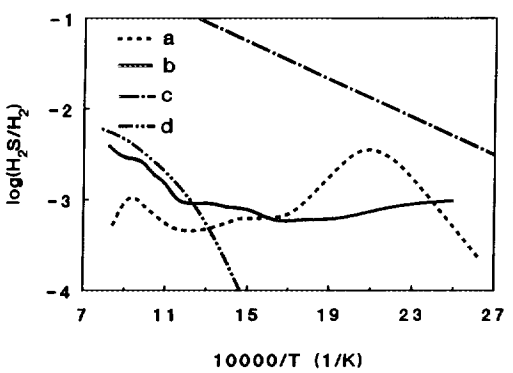

FIG. 13. Comparison of the experimental H_2S/H_2 ratio during the TPR experiments of sulfided Ni(2.6)/Al-773 (a) and Ni(2.9)/W(2.3)/Al-773 (b) with the theoretical H_2S/H_2 ratio at thermodynamic equilibrium of NiS with Ni_3S_2 (c) and Ni_3S_2 and Ni metal (d).

Analogously to Ni(x)/Al-773, sulfiding of Ni(x)/W(2.3)/Al-773 resulted in the complete disappearance of the H_2 consumption of the dispersed NiO phase (in TPR), confirming that this phase is completely sulfidable at 673 K.

Since the interpretation is rather complicated, the various phases present after sulfiding at 673 K are indicated in the TPR-S pattern of the Ni(2.0)/W(2.3)/Al-773 catalysts (Fig. 14). The UV peak at 1200 K is ascribed to the reduction of WS_2. The amount of H_2 required to reduce this phase is indicated in the TCD pattern. The remaining H_2 consumption at 1200 K is caused by reduction of dispersed WO_3. Between 800 and 1100 K reduction of Ni_3S_2 takes place. Despite the fact that reduction of NiWS is not observed due to sintering ($NiWS \rightarrow Ni_3S_2 + WS_2$), the reduction of NiWS is indicated. The amount of H_2 consumed to reduce Ni_3S_2 is indicated in the TCD pattern. The additional amount of H_2 is assigned to reduction of nonsulfided $NiAl_2O_4$ and NiWOAl species. Analogous to the TPR-S patterns of the W(2.3)/Al catalysts the H_2S production and corresponding H_2 consumption in region II are the result of recombination of S–H groups and reaction of H_2 and S–H groups. Similar to Ni(x)/Al and W(2.4)/Al catalysts, reduction of S_x species is observed in region I. The reduction occurs at a temperature lower than with Ni(x)/Al, and also slightly lower than with

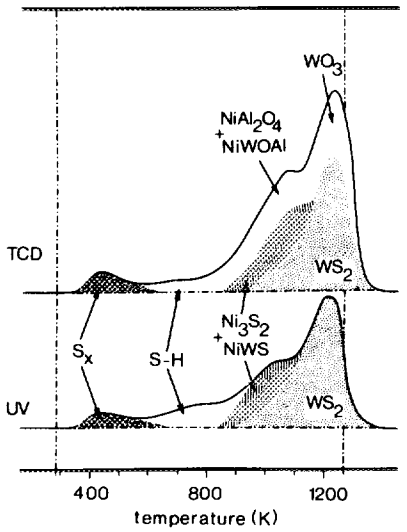

FIG. 14. The various phases present after sulfiding NiW catalysts at 673 K are indicated in the TPR-S pattern of Ni(2.0)/W(2.3)/Al.

W(2.3)/Al catalysts. Because reduction of S might be an elementary step in HDS, the reduction rate of the S_x species might be correlated to the desulfurisation activity. The order of activity of Ni, W, and Ni–W based catalysts was Ni < W ≪ Ni–W (30). The reduction temperature of S_x decreases in the same order. However, the reduction temperature of these species differs only slightly for the W and Ni–W catalysts, whereas the activity of these catalysts differs by one order of magnitude. Hence, the reduction temperature of S_x and HDS activity are only weakly correlated. Thus it is not likely that the reaction of S with H_2 to H_2S on W and NiW catalysts is the rate-limiting step in HDS. The analogous conclusion has been drawn for Co–Mo catalysts (15).

CONCLUSIONS

Detailed information about the sulfidability of the various species in alumina-supported Ni, W, and Ni–W catalysts is obtained by combination of the TPR patterns of the oxidic and sulfidic catalysts.

The following phases have been found in the oxidic catalysts: a highly dispersed NiO surface phase, surface, and subsurface $NiAl_2O_4$-like phases, dispersed WO_3, a mixed $NiO–WO_3$ phase (NiWOAl) and dispersed $NiWO_4$ crystallites.

The major part of the dispersed species present on Ni/Al catalysts, calcined above 773 K, is not sulfidable at industrial sulfiding temperatures (<673 K). Only the dispersed Ni^{2+} surface phase is completely sulfidable at this temperature.

W/Al catalysts (2.4 at/nm^2) are only partly sulfided at commonly applied sulfiding temperatures; the degree of sulfiding increased from ±24 to 95% upon an increase of the sulfiding temperature from 573 to 873 K.

The mixed Ni–W phase is partly sulfided at 673 K, depending on the speciation of the Ni ions; Ni ions located at the WO_3 monolayer are sulfided, while Ni ions incorporated in the WO_3 monolayer are not. The sulfidability of the WO_3 monolayer is only slightly affected by the presence of Ni. $NiWO_4$ which is formed after calcination at 1073 K is not sulfidable at 673 K.

Reduction of bulk WS_2 took place in one step between 1000 and 1270 K, and the rate was determined by thermodynamics. Bulk NiS reduced in two steps, viz. NiS to Ni_3S_2, and Ni_3S_2 to Ni^0. The rate of the first step was determined by kinetics and that of the second by thermodynamics.

WS_2 slabs formed during sulfiding of W/Al catalysts are reduced above 1000 K at a rate determined by bulk thermodynamics. The reduction of the NiS_{1+x} species is divided into two categories, viz., the reduction of microcrystalline NiS_{1+x}, which is reduced in two steps similar to the reduction of bulk NiS, and ultra-dispersed nickel sulfide which is reduced in one step above 900 K. The reduction of the NiWS phase is not observed due to sintering during the temperature program, leading to Ni_3S_2 and WS_2.

After sulfiding at 673 K, a small part of the sulfur is present as S–H groups.

On all catalysts, the reduction of a nonstoichiometric phase (S_x) is observed, which is chemisorbed on coordinatively unsaturated sites. The chemisorption of these sulfur atoms is not restricted to sulfides but can also take place on oxidic material. Despite the fact that the reduction of these sulfur species took place below HDS reaction temperatures, only a weak correlation existed between the HDS activity and the reduction temperature. Under HDS conditions, hydrogenation of S is not the rate-limiting step for alumina-supported NiW catalysts.

ACKNOWLEDGMENT

Financial support from the EC under contract number 704F0049 is gratefully acknowledged.

REFERENCES

1. Lacroix, M., Vrinat, M., and Breysse, M., *Appl. Catal.* **21,** 73 (1986).
2. Salvati, L., Makovsky, L. E., Stencel, J. M., Brown, F. R., and Hercules, D. M., *J. Phys. Chem.* **86,** 3700 (1981).
3. Breysse, M., Bachelier, J., Bonnelle, J. P., Cattenot, M., Cornet, D., Décamp, T., Duchet, J. C., Durand, R., Engelhard, P., Fréty, R., Gachet, C., Geneste, P., Grimblot, J., Gueguen, C., Kasztelan, S., Lacroix, M., Lavalley, J. C., Leclercq, C., Moreau, C., de Mourgues, L., Olivé, J. L. Payen, E., Portefaix, J. L., Toulhoat, H., and Vrinat, M., *Bull. Soc. Chim. Belg.* **96,** 829 (1987).

4. Duchet, J. C., Lavalley, J-C., Housni, S., Okafi, D., Bachelier, J., Lakhdar, M., Mennour, A., and Cornet, D., *Catal. Today* **4,** 71 (1988).
5. Blanchard, L., Grimblot J., and Bonnelle, J. P., *J. Catal.* **98,** 229 (1986).
6. Shepelin, A. P., Zhdan, P. A., Burmistrov, V. A., Startsev, A. N., and Yermakov, Y. I., *Appl. Catal.* **11,** 29 (1984).
7. Scheffer, B., Molhoek, P., and Moulijn, J. A., *Appl. Catal.* **46,** 11 (1989).
8. Scheffer, B., Mangnus, P. J., and Moulijn, J. A., *J. Catal.* **121,** 18 (1990).
9. Scheffer, B., Heijinga, J. J., and Moulijn, J. A., *J. Phys. Chem.* **91,** 4572 (1987).
10. Ng, K. T., and Hercules, D. M., *J. Phys. Chem.* **80,** 2094 (1976).
11. Mangnus, P. J., Scheffer, B., and Moulijn, J. A., *Prep.—Am. Chem. Soc., Div. Pet. Chem.* **32,** 329 (1987).
12. Arnoldy, P., Franken, M. C., Scheffer, B., and Moulijn, J. A., *J. Catal.* **96,** 381 (1985).
13. Scheffer, B., van Oers, E. M., Arnoldy, P., de Beer V. H. J., and Moulijn, J. A., *Appl. Catal.* **25,** 303 (1986).
14. Scheffer, B., Dekker, N. J. J., Mangnus, P. J., and Moulijn, J. A., *J. Catal.* **121,** 31 (1990).
15. Mangnus, P.J., Riezebos, A., van Langeveld, A. D., and Moulijn, J. A., submitted for publication in *J. Catal.*
16. Arnoldy, P., and Moulijn, J. A., *J. Catal.* **93,** 38 (1985).
17. Thomas, R., de Beer, V. H. J., and Moulijn, J. A., *Bull. Soc. Chim. Belg.* **90,** 1349 (1981).
18. Rosenqvist, T., *J. Iron Steel Inst., London* **176,** 37 (1954).
19. Barin, I., and Knacke, O., *in* "Thermochemical Properties of Inorganic Substances," supplement. Springer-Verlag, Berlin, 1977.
20. Breysse, M., Cattenot, M., Decamp, T., Fréty, R., Gachet, C., Lacroix, L., Leclercq, C., de Mourges, L., Portefaix, J. L., Vrinat, J., Houari, M., Grimblot, J., Kasztelan, S., Bonnelle, J. P., Housni, S., Bachelier, J., and Duchet, J. C., *Catal. Today* **4,** 39 (1988).
21. Payen, E., Kasztelan, S., and Grimblot, J., *J. Mol. Struct.* **174,** 71 (1988).
22. Payen, E., Kasztelan, S., Grimblot, J., and Bonnelle, J. P., *Catal. Today* **4,** 57 (1988).
23. Ramachandran, R., and Massoth, F. E., *Can. J. Chem. Eng.* **60,** 17 (1982).
24. Puxley, P. C., Kitchener, I. J., Komodromos, C., and Parkyns, N. D., *in* "Preparation of Catalysts III" (G. Poncelet, P. Grange, and P. A. Jacobs, Eds.), p. 237. Elsevier, Amsterdam, 1983.
25. de Korte, P. H. M., Doesburg, E. B. M., de Winter, C. P. J., and van Reijen, L. L., *Solid State Ionics* **16,** 73 (1985).
26. Bachelier, J., Duchet, J. C., and Cornet, D., *Bull. Soc. Chim. Fr.* **3–4,** I-112 (1978).
27. Bartholomew, C. H., Agrawal, P. K., and Katzer, J. R., *Adv. Catal.* **31,** 135 (1982).
28. Ouafi, D., Mauge, F., Lavalley, J. C., Payen, E., Kasztelan, S., Houari, M., Grimblot, J., and Bonnelle, J-P., *Catal. Today* **4,** 23 (1988).
29. Iannibello, A., Marengo, S., Morelli, G., and Tittarelli, P., *in* "Climax 4th Intern. Conf. on Chemistry and Uses of Molybdenum" (H. F. Barry and P. C. H. Mitchell, Eds.), p. 256. Ann Arbor, Michigan, 1982.
30. Scheffer, B., Ph.D. thesis, University of Amsterdam, 1988.